Published in final edited form as:
Dev Biol. 2009 December 15; 336(2): 266–279. doi:10.1016/j.ydbio.2009.10.007.

Forkhead Box M1 Transcriptional Factor is Required for Smooth Muscle Cells during Embryonic Development of Blood Vessels and Esophagus

Vladimir Ustiyan[1], **I-Ching Wang**[1], **Xiaomeng Ren**[1], **Yufang Zhang**[1], **Jonathan Snyder**[1], **Yan Xu**[1], **Susan E. Wert**[1], **James L. Lessard**[2], **Tanya V. Kalin**[1], and **Vladimir V. Kalinichenko**[1,2,*]

[1]Division of Pulmonary Biology, Perinatal Institute of the Cincinnati Children's Hospital Research Foundation, 3333 Burnet Ave., Cincinnati, OH 45229.

[2]Division of Developmental Biology, Perinatal Institute of the Cincinnati Children's Hospital Research Foundation, 3333 Burnet Ave., Cincinnati, OH 45229.

Abstract

The Forkhead Box m1 (Foxm1 or Foxm1b) transcription factor (previously called HFH-11B, Trident, Win, or MPP2) is expressed in a variety of tissues during embryogenesis, including vascular, airway and intestinal smooth muscle cells (SMC). Although global deletion of Foxm1 in *Foxm1*$^{-/-}$ mice is lethal in the embryonic period due to multiple abnormalities in the liver, heart and lung, the specific role of Foxm1 in SMC remains unknown. In the present study, Foxm1 was deleted conditionally in the developing SMC (*smFoxm1*$^{-/-}$ mice). The majority of *smFoxm1*$^{-/-}$ mice died immediately after birth due to severe pulmonary hemorrhage, and structural defects in arterial wall and esophagus. Although Foxm1 deletion did not influence SMC differentiation, decreased proliferation of SMC was found in *smFoxm1*$^{-/-}$ blood vessels and esophagus. Depletion of Foxm1 in cultured SMC caused G2 arrest and decreased numbers of cells undergoing mitosis. Foxm1-deficiency *in vitro* and *in vivo* was associated with reduced expression of cell cycle regulatory genes, including cyclin B1, Cdk1-activator Cdc25b phosphatase, Polo-like 1 and JNK1 kinases, and cMyc transcription factor. Foxm1 is critical for proliferation of smooth muscle cells and is required for proper embryonic development of blood vessels and esophagus.

Keywords

winged helix DNA binding domain; Forkhead transcription factor; Foxm1; vascular development; esophagus; smooth muscle cells

INTRODUCTION

Embryonic development of blood vessels depends on proper vasculogenesis (formation of blood vessels *de novo*) and angiogenesis (branching of preexisting blood vessels). While the

***Correspondence** to: Dr. Vladimir V. Kalinichenko, Division of Pulmonary Biology, Cincinnati Children's Hospital Research Foundation, 3333 Burnet Ave., MLC 7009, Cincinnati, OH 45229. Vladimir.Kalinichenko@cchmc.org.

majority of vascular cell types develop from the mesoderm (Saint-Jeannet et al., 1992), smooth muscle cells (SMC) may arise from multiple origins, including mesodermal cells, neural crest cells, hematopoietic stem cells, pericytes and endothelial cells (Thayer et al., 1995; Gittenberger-de Groot et al., 1999; Hao et al., 2003). In contrast to terminally differentiated skeletal and cardiac muscle cells, mature SMC retain the ability to change their phenotype in response to changing environment conditions (Halayko and Solway, 2001). Several signaling pathways are critical for proper development of blood vessels, including vascular endothelial growth factor (VEGF), angiopoietins, transforming growth factor β (TGF-β), fibroblast growth factors (FGFs), platelet-derived growth factor (PDGF), Ephrin/Eph receptor, Sonic hedgehog (Shh)/ Patch, and Delta-ligand/ Notch-receptors (Carmeliet et al., 1996; Rossant and Howard, 2002; Chi et al., 2007), as well as both canonical (Wnt7b) and Ca^{2+}-dependent (Wnt4) Wnt-signaling pathways (Shu et al., 2002; Itaranta et al., 2006). These signaling proteins regulate proliferation, differentiation and migration of SMC in the vascular wall by inducing expression of transcription factors critical for regulation of SM-specific gene promoters. These transcription factors include the serum response factor (SRF), myocardin and myocardin-related transcriptional factors that act as SRF activators to induce expression of SRF target genes (Wang et al., 2001; Camoretti-Mercado et al., 2003; Pipes et al., 2006). Development of blood vessels also depends on MEF2B, P311 (C5orf13), MRF2 (ARID5B) and GATA4 transcription factors that are essential for differentiation of mesenchymal cells toward SMC cell lineage (Katoh et al., 1998; Belaguli et al., 2000; Pan et al., 2002; Watanabe et al., 2002; Kumar and Owens, 2003).

The Forkhead Box (Fox) proteins are an extensive family of transcription factors that share homology in the Winged Helix/*Forkhead* DNA binding domain (Clark et al., 1993; Clevidence et al., 1993; Kaestner et al., 1993). Foxm1 transcription factor (previously known as HFH-11B, Trident, Win, or MPP2) is expressed in all tissues during embryogenesis but its expression in adult mice is restricted to intestinal crypts, thymus and testes (Korver et al., 1997; Ye et al., 1997). During organ injury, Foxm1 expression is induced in a variety of cell types, including epithelial, endothelial and smooth muscle cells (Ye et al., 1997; Kalinichenko et al., 2003). Foxm1 expression is increased in tumor cells during progression of liver, lung, colon and prostate cancers (Kalinichenko et al., 2004; Kalin et al., 2006; Kim et al., 2006; Yoshida et al., 2007). In our previous studies we demonstrated that *Foxm1*$^{-/-}$ mice die *in utero* between embryonic day 13.5 (E13.5) and E16.5 due to multiple abnormalities in development of the embryonic liver, lung, and heart (Krupczak-Hollis et al., 2004; Kim et al., 2005a; Ramakrishna et al., 2007). Abnormal accumulation of polyploid cells, resulting from diminished DNA replication and failure to enter mitosis, was observed in these *Foxm1*$^{-/-}$ mouse organs (Korver et al., 1998; Krupczak-Hollis et al., 2004; Ramakrishna et al., 2007). Foxm1 is required for differentiation of hepatoblast precursor cells toward the biliary epithelial cell lineage, and *Foxm1*$^{-/-}$ livers fail to form intrahepatic bile ducts (Krupczak-Hollis et al., 2004). Likewise, *Foxm1*$^{-/-}$ embryos exhibit defects in differentiation of pulmonary mesenchyme into mature capillary endothelial cells during the canalicular stage of lung development (Kim et al., 2005a).

Given the importance of Foxm1 for differentiation and proliferation of many cell lineages during embryonic development, organ injury and carcinogenesis, several recent studies began to address cell-specific roles of Foxm1 using conditional knockout mouse models. Hepatocyte-specific deletion of Foxm1 in Albumin-Cre *Foxm1*$^{fl/fl}$ mice prevented formation of hepatocellular carcinoma (HCC) in adult mice by inducing $p27^{kip1}$ tumor suppressor in HCC tumor cells and normal hepatocytes (Kalinichenko et al., 2004). In response to the inflammatory mediator LPS, mice with endothelial-specific Foxm1 deletion (Tie2-Cre *Foxm1*$^{fl/fl}$ mice) displayed significantly increased lung vascular permeability and markedly increased mortality (Zhao et al., 2006). A conditional deletion of Foxm1 from precursors of cerebellar granule neurons caused a delay in brain development by interfering with Shh-induced

neuroproliferation (Ueno et al., 2008). Mice with pancreatic-specific deletion of Foxm1 displayed severe abnormalities in postnatal β-cell mass expansion, causing impaired islet function and diabetes by 9 week of age (Zhang et al., 2006). These mice also exhibited specific impairments in β-cell mass regeneration and islet growth after partial pancreatectomy, with reduced proliferation of α- and β-cells but no impairments in acinar or ductal cell proliferation (Ackermann Misfeldt et al., 2008). In our recent studies (Kalin et al., 2008), Foxm1 was deleted conditionally in the respiratory epithelium during lung development (*SPC-rtTA/ TetO-Cre Foxm1*$^{fl/fl}$ mice). Deletion of Foxm1 in the respiratory epithelium did not alter epithelial proliferation but inhibited lung maturation and caused respiratory failure after birth (Kalin et al., 2008). Maturation defects in Foxm1-deficient lungs were associated with a delay of type I cell differentiation and decreased expression of surfactant-associated proteins A, B, C, and D, indicating that Foxm1 is critical for surfactant homeostasis and lung maturation prior to birth and is required for adaptation to air breathing (Kalin et al., 2008). Although Foxm1 plays distinct roles in differentiation and proliferation in various cell lineages, the specific role of Foxm1 in smooth muscle cells remains unknown.

In this study, we used mouse embryos to demonstrate that Foxm1 is expressed in vascular smooth muscle and airway smooth muscle cells as well as in smooth muscle layers of esophagus, stomach and intestine. To investigate the role of Foxm1 in smooth muscle cells *in vivo*, we generated transgenic mice in which Foxm1-floxed allele was conditionally deleted using Cre recombinase transgene driven by a smooth muscle myosin heavy chain promoter (smMHC-Cre *Foxm1*$^{fl/fl}$, or *smFoxm1*$^{-/-}$ mice). We demonstrated that a majority of *smFoxm1*$^{-/-}$ mice died immediately after birth due to severe pulmonary hemorrhage, structural defects in arterial wall, and esophageal abnormalities. Although Foxm1 deletion did not influence differentiation of smooth muscle cells, decreased cellular proliferation was observed in muscle layers of embryonic blood vessels and esophagus. In vitro experiments demonstrated that siRNA-mediated depletion of Foxm1 in cultured smooth muscle cells caused G2 arrest and decreased numbers of cells undergoing mitosis. Depletion of Foxm1 *in vitro* and *in vivo* was associated with reduced expression of cell cycle regulatory genes, including cyclin B1, Cdk1-activator Cdc25b phosphatase, Polo-like 1 and JNK1 kinases, and cMyc transcription factor. Our studies suggest that Foxm1 is required for proper development of blood vessels and esophagus by regulating smooth muscle genes essential for the cell cycle regulation.

MATERIALS AND METHODS

Mouse strains

We previously described the generation of *Foxm1*$^{flox/flox}$ (*Foxm1*$^{fl/fl}$) mice, which contain LoxP sequences flanking DNA binding and transcriptional activation domains of the *Foxm1* gene (Krupczak-Hollis et al., 2004). The *Foxm1*$^{fl/fl}$ mice were bred for 10 generations into C57Bl/6 mouse genetic background. The *Foxm1*$^{fl/fl}$ female mice were bred with *smMHC-Cre-GFP*$^{tg/-}$ C57Bl/6 male mice (obtained from Dr. Kotlikoff, Cornell University, (Xin et al., 2002)) to generate the *smMHC-Cre-GFP*$^{tg/-}$ *Foxm1*$^{fl/fl}$ double transgenic mice (smooth muscle-specific Foxm1 knockout mice or *smFoxm1*$^{-/-}$). Although a majority of *smFoxm1*$^{-/-}$ embryos died immediately after birth, 13% of *smFoxm1*$^{-/-}$ mice survived through birth and were capable of mating. *Foxm1*$^{fl/fl}$ littermates lacking the *smMHC-Cre-GFP* transgene were used as controls. Further controls included double-heterozygous *smMHC-Cre-GFP*$^{tg/-}$ *Foxm1*$^{fl/+}$ mice. No embryonic abnormalities were observed in control mice. *smMHC-Cre-GFP*$^{tg/-}$ *Foxm1*$^{fl/fl}$ mice were bred with either TOPGAL transgenic mice (obtained from J. Whitsett's lab, Cincinnati Children's Hospital Medical Center) or R26R reporter mice (Rosa26-LoxP-stop-LoxP-β-galactosidase mice; purchased from Jackson Lab) to study canonical Wnt signaling or Cre-mediated recombination, respectively. Animal studies were

reviewed and approved by the Animal Care and Use Committee of Cincinnati Children's Hospital Research Foundation.

Immunohistochemical staining, *in situ* hybridization and laser capture microdissection

smFoxm1$^{-/-}$ and control *Foxm1*$^{fl/fl}$ embryos were harvested, fixed overnight with 10% buffered formalin, and then embedded into paraffin blocks. Paraffin 5 μm sections were either used for immunohistochemistry or stained with hematoxylin and eosin (H&E) for morphological examination as described (Kim et al., 2005b). The following antibodies were used for immunostaining: Cre (1:25,000; #69050-3; Novagen); Ki-67 (1:500; clone Tec-3; Dako); GFP (1:15,000; clone JL-8; Clontech); activated caspase 3 (1:200; 5A1; Cell signaling), α-smooth muscle actin (αSM; 1:15,000; clone 1A4; Sigma), γ-smooth muscle actin (γSM; 1:500; clone B4; Seven Hills Bioreagents, Cincinnati, OH), smooth muscle calponin (1:5000; clone hCP; Sigma), smooth muscle myosin heavy chain (1:250; clone HSM-V; Sigma), Pecam-1 (1:300, clone MEC 13.3, Pharmingen), Foxa2 (1:2,000, Seven Hills Bioreagents, Cincinnati, Ohio), proSPC (1:1,500, AB-3428, Chemicon International), CCSP (1:1,000, a gift from Dr. Stripp, Duke University), and MyoD (1:20, NCL-MyoD1, Vision Bio Systems Novocastra). Antibody-antigen complexes were detected using biotinylated secondary antibody followed by avidin-horseradish peroxidase (HRP) complex, and DAB substrate (Vector Labs, Burlingame, CA). Sections were counterstained with nuclear fast red. For co-localization experiments, paraffin sections were stained with FITC-labeled αSM antibodies (green fluorescence) followed by immunostaning with antibodies against either cleaved caspase 3 or Ki-67 that were detected by TRITC-labeled secondary antibodies (red fluorescence). DAPI was used as a counterstain. Fluorescent images were obtained using a Zeiss Axioplan2 microscope equipped with an AxioCam MRm digital camera and AxioVision 4.3 Software (Carl Zeiss Microimaging, Thornwood, NY).

Paraffin sections were also used for *in situ* hybridization with ^{35}S-labeled antisense riboprobe specific to 1649 – 1947 bp region of the mouse Foxm1 mRNA as described (Kalin et al., 2008). We used frozen E16.5 sections to perform laser capture microdissection of aortic tissue in *smFoxm1*$^{-/-}$ and control *Foxm1*$^{fl/fl}$ mice. The Veritas Microdissecting System (Molecular Devices, Sunnyvale, CA) was used for the laser capture microdissection experiments accordingly to protocols supplied by the manufacturer.

siRNA transfection, flow cytometry and PH3 staining in cultured HAVSMC cells

Human aortic vascular smooth muscle cells (ATCC cell line *T/G HA-VSMC*) were cultured in F-12K medium with supplements recommended by ATCC. In order to inhibit Foxm1 expression in HAVSMC cells, we used a 21-nucleotide short interfering RNA (siRNA) duplex specific to 1066-1084 nucleotide region of the human Foxm1 cDNA (siFoxm1, 5’-gga cca cuu ucc cua cuu u-3’). Foxm1 siRNA containing symmetric 2-Uracil (U) 3’ overhangs was designed and synthesized using Dharmacon Research algorithm (Kim et al., 2006). We transfected 100 nM of either siFoxm1 or mutant siFoxm1 (mutFoxm1; mutated nucleotides are indicated by capital letters, 5’-gga ccU GuA uGc Gua cAu u-3’) duplexes into human HAVSMC cells using Lipofectamine™ 2000 reagent (Invitrogen) in serum free tissue culture media as described previously (Wang et al., 2005a; Kim et al., 2006). HAVSMC cells were harvested at 72 hr after transfection for total RNA preparation or propidium iodide (PI) staining. PI-stained HAVSMC cells were analyzed by flow cytometry to determine numbers of cells in different stages of the cell cycle as described previously (Wang et al., 2005a). The flow cytometry and analysis were performed in the Flow cytometry core facility of Cincinnati Children's Hospital Research Foundation. In separate experiments, HAVSMC cells undergoing either G0/ G1 or G2/ M phase of the cell cycle were identified using Vybrant DyeCycle™ Violet stain (Invitrogen) according to manufacturer's recommendations. Stained cells were sorted using a 5-laser FACSAria II flow cytometer (BD Biosciences). The cells in G0/G1 and

G2/M phase were harvested into collection tubes filled with RLT RNA lysis buffer, and then used to prepare total RNA. For PH3 staining, siRNA-transfected HAVSMC cells were fixed with 10% buffered formalin and immunostained with antibodies against phospho-Histone H3 (PH3; 1:100 dilution; #06-570; Upstate) to visualize cells undergoing mitosis as described (Wang et al., 2005a).

Affymetrix cDNA array analysis and quantitative real-time RT-PCR (qRT-PCR)

Total RNA was prepared from either siFoxm1-transfected or mock-transfected HAVSMC cells using RNA-STAT-60 (Tel-Test "B" Inc. Friendswood, TX). Synthesis of human HAVSMC cDNAs with CyDye nucleotides (Cy3 and Cy5), hybridization of Affymetrix GeneChip® Human Genome U133 plus 2.0 array, scanning, and analysis of cDNA Microarrays were performed by the Functional Genomics Facility at the University of Chicago (Chicago, IL). Data were deposited to GEO public database (http://www.ncbi.nlm.nih.gov/geo/query/acc.cgi?acc=GSE17543; accession # GSE17543). Data were analyzed using Genespring 7.2 (Silicon Genetics). A volcano plot was used to identify significance and magnitude of gene expression changes with a minimum set as 2-fold as previously described (Dave et al., 2006). Gene expression profile was also subjected to an additional filter and classified according to Gene Ontology classification on Biological Process using the publicly available web-based tool David (database for annotation, visualization, and integrated discovery) (Dennis et al., 2003). The Fisher exact test was used to calculate the probability of each gene ontology category among all genes included in the array. To avoid individual variations, we combined 10 μg of RNA from three distinct HAVSMC cell cultures for each group. Expression levels of 421 genes were decreased > 2.0-fold in siFoxm1-transfected cells compared to mock-transfected HAVSMC cells. Expression levels of 27 genes were increased > 2.0-fold in siFoxm1-transfected cells.

To verify expression levels of selected genes, we performed qRT-PCR analysis using a StepOnePlus Real-Time PCR system (Applied Biosystems, Foster City, CA) as described (Kalin et al., 2008). Samples were amplified with TaqMan Gene Expression Master Mix (Applied Biosystems) combined with inventoried TaqMan gene expression assays for the gene of interest (Table 1). Reactions were analyzed in triplicates and expression levels were normalized to β-actin. Total RNA was also prepared from laser-captured E16.5 aortic tissue of either *smFoxm1*$^{-/-}$ or control *Foxm1*$^{fl/fl}$ embryos and then analyzed by qRT-PCR. Three embryos were used in each group.

Statistical analysis

Student's T-test was used to determine statistical significance. P values ≤ 0.05 were considered significant. Values for all measurements were expressed as the mean ± standard deviation (SD).

RESULTS

Conditional deletion of Foxm1 in smooth muscle cells causes a perinatal lethality

Previous studies have demonstrated that Foxm1 is expressed in a variety of cell types during embryogenesis (Ye et al., 1997; Kalin et al., 2008). To detect Foxm1 expression in developing smooth muscle cells, *in situ* hybridization was performed with Foxm1-specific anti-sense riboprobe. In E15.5 mouse embryos, Foxm1 mRNA was detected in vascular smooth muscle cells of arteries (Fig. 1A-C) as well as in smooth muscle cells underlying the developing esophagus, trachea, bronchi, stomach and intestine (Fig. 1A-F and data not shown). In adult mice, Foxm1 expression was observed in epithelium of intestinal crypts (Fig. 1G-H). Foxm1 mRNA was not detected in smooth muscle cells of intestine, bronchi or blood vessels of the adult mice (Fig. 1G-H and data not shown). These data demonstrate that Foxm1 is expressed

in different populations of smooth muscle cells during embryonic development but its expression is extinguished in adult smooth muscle cells.

To determine whether Foxm1 is required for smooth muscle cells during embryonic development, we generated double-transgenic mice containing LoxP-flanked exons 4-7 of the *Foxm1* gene (*Foxm1*$^{fl/fl}$) and Cre recombinase transgene driven by smooth muscle myosin heavy chain promoter (smMHC-Cre-GFP, (Xin et al., 2002)). Previous studies demonstrated that using this smMHC-Cre-GFP transgenic mouse line, Cre-mediated recombination occurs in all populations of smooth muscle cells beginning from E12.5 (Xin et al., 2002). The smooth muscle-specific expression of Cre recombinase causes deletion of exons 4, 5, 6 and 7, which encode the DNA binding and transcriptional activation domains of the *Foxm1* protein (Fig. 1I), to produce smooth muscle-specific *Foxm1* knockout mice (smMHC-Cre-GFP $^{tg/-}$/ *Foxm1*$^{fl/fl}$ or *smFoxm1*$^{-/-}$). In *smFoxm1*$^{-/-}$ newborn mice, body weight, and lung to body weight ratio were unchanged (data not shown). However, deletion of *Foxm1* caused a perinatal lethality in 87% of *smFoxm1*$^{-/-}$ mice within the first 24 hours after birth (Table 2). No perinatal lethality was observed in control *Foxm1*$^{fl/fl}$ littermates, or double-heterozygous smMHC-Cre-GFP $^{tg/-}$/ *Foxm1*$^{fl/+}$ newborn mice (data not shown). When assessed prior to birth, *smFoxm1*$^{-/-}$ embryos were present as Mendelian inheritance (Table 2), indicating that the Foxm1 function in smooth muscle cells was not required for fetal survival *in utero*, but was critical for survival immediately after birth.

To determine whether Cre recombination in *smFoxm1*$^{-/-}$ embryos occurred prior to the perinatal lethality, we bred *smFoxm1*$^{-/-}$ mice with R26R reporter mice to generate *smFoxm1*$^{-/-}$/ R26R embryos, which were stained for β-galactosidase (β-gal) activity. Although β-gal activity was not detected in control *Foxm1*$^{fl/fl}$/ R26R embryos at E15.5 (Fig. 1L), β-gal activity was observed in Foxm1-deficient smooth muscle cells of E15.5 arteries, esophagus, stomach, trachea, bronchi, and intestine (Fig. 1M-P and data not shown). Furthermore, to detect the presence of Cre protein in smooth muscle cells, *smFoxm1*$^{-/-}$ and control *Foxm1*$^{fl/fl}$ embryos were immunostained with antibodies against Cre recombinase. Although Cre was not expressed in *Foxm1*$^{fl/fl}$ embryos (Fig. 1T), Cre protein was detected in smooth muscle cells surrounding esophagus, stomach, intestine, and pulmonary airways of E15.5 *smFoxm1*$^{-/-}$ embryos (Fig. 1U-W and data not shown), which is consistent with β-gal activity in *smFoxm1*$^{-/-}$/ R26R embryos (Fig. 1L-P). Finally, specific expression of Cre transgene in *smFoxm1*$^{-/-}$ smooth muscle cells was also confirmed by immunostaining with antibodies against GFP (Fig. 1R-S and data not shown), a reporter protein expressed under control of smMHC promoter in *smFoxm1*$^{-/-}$ embryos (Fig. 1I). Altogether, these results demonstrate that both Cre-mediated recombination and expression of Cre transgene occurred in smooth muscle cells of *smFoxm1*$^{-/-}$ embryos prior to perinatal lethality. Interestingly, although a mosaic Cre recombination was detected in atriums of Foxm1 mutant hearts as wells as in cardiac regions directly adjacent to aorta and pulmonary trunk, no structural abnormalities were observed in these heart regions (Fig. 1Q and data not shown).

Foxm1 is required for development of esophagus

Since Foxm1 is expressed in esophageal, bronchial and intestinal muscle layers (Fig. 1A-F), histological analysis of these organs was performed in *smFoxm1*$^{-/-}$ embryos. Embryonic esophageal muscle is composed of outer longitudinal and inner circumferential layers, both of which express Cre recombinase transgene in *smFoxm1*$^{-/-}$ mutant mice (Fig. 1M and 1V). Histological structure of esophagus was similar in *smFoxm1*$^{-/-}$ and control *Foxm1*$^{fl/fl}$ littermates at E15.5 (Fig. 2A-B). At E18.5, esophageal muscle in *smFoxm1*$^{-/-}$ mutants appeared underdeveloped, and a progressive loss of mesenchymal cells became apparent (Fig. 2E and 2J). Significantly diminished thickness of esophageal muscle was found in *smFoxm1*$^{-/-}$ E18.5 embryos (Fig. 2V). No structural abnormalities were observed in either

Foxm1$^{fl/fl}$ or *smMHC-Cre-GFP*$^{tg/-}$ embryos (Fig. 2C-D and 2H-I). In *smFoxm1*$^{-/-}$ newborn mice, the entire esophagus contained very thin muscular layers fused together (Fig. 2F-G). The structural abnormalities of the esophagus can interfere with proper functions of the gastrointestinal system, contributing to perinatal lethality in *smFoxm1*$^{-/-}$ newborn mice. Interestingly, no intestinal, bronchial or stomach defects were found in *smFoxm1*$^{-/-}$ embryos or newborn mice (Figs. 2K-O and P-R), indicating different requirements in Foxm1 function in different populations of developing smooth muscle cells. Finally, normal expression of CCSP (Clara cell marker) and proSPC (type II cell marker) was observed in *smFoxm1*$^{-/-}$ E18.5 airways when compared to either *Foxm1*$^{fl/fl}$ or *smMHC-Cre-GFP*$^{tg/-}$ embryos (Fig. 2P-U). These results suggest that Foxm1 deficiency does not influence the development of different populations of epithelial cells in pulmonary airways.

Foxm1 is required for proper development of blood vessels

Histological examination of the *smFoxm1*$^{-/-}$ newborn mice revealed extensive pulmonary hemorrhage with red blood cells present in bronchioles and peripheral pulmonary saccules (Fig. 3A-B). Pulmonary arteries from *smFoxm1*$^{-/-}$ mice displayed multiple hernias in arterial walls, disruption of vascular muscle layers, and accumulation of large cells with round nuclei (Fig. 3G-L), the latter of which is a hallmark of Foxm1 deficiency (Korver et al., 1998; Krupczak-Hollis et al., 2004; Ramakrishna et al., 2007). Morphological evidence of vascular leakage from perforated pulmonary arteries was also detected in *smFoxm1*$^{-/-}$ newborn mice (Fig. 3E-F). Thus, the structural abnormalities of the arterial wall can compromise vascular integrity and contribute to perinatal lethality in *smFoxm1*$^{-/-}$ newborn mice. Interestingly, hemorrhage was not observed in the liver, gut, brain and skeletal muscle of the *smFoxm1*$^{-/-}$ newborn mice, and the heart structure in *smFoxm1*$^{-/-}$ mice was normal (data not shown). Since lung hemorrhage was not detected in *smFoxm1*$^{-/-}$ mutants prior to birth (data not shown), these results indicate that the hemorrhaging phenotype was concomitant with the increased pulmonary arterial blood flow that occurs following birth.

Published studies demonstrated that *Wnt7b*$^{-/-}$ mice displayed extensive pulmonary hemorrhage, perinatal lethality and structural abnormalities in vascular smooth muscle (Shu et al., 2002), a phenotype similar to *smFoxm1*$^{-/-}$ mice (Fig. 3A-L). The vascular defects in *Wnt7b*$^{-/-}$ mice were attributed to a disruption of canonical Wnt signaling in vascular smooth muscle cells (Shu et al., 2002; Wang et al., 2005b). Therefore, the vascular abnormalities in *smFoxm1*$^{-/-}$ mutants could occur due to diminished activity of canonical Wnt signaling pathway. To visualize the canonical Wnt signaling in Foxm1-deficient embryos, we bred *smFoxm1*$^{-/-}$ mice with TOPGAL transgenic mice to produce TOPGAL$^{tg/-}$/ *smFoxm1*$^{-/-}$ embryos. The TOPGAL$^{tg/-}$/ *smFoxm1*$^{-/-}$ embryos were stained for β-gal activity and then compared to control TOPGAL$^{tg/-}$/ *Foxm1*$^{fl/fl}$ littermates. In E12.5 and E13.5 embryos, β-gal activity was detected in pulmonary arteries, bronchi, stomach, cartilage, and aortic outflow and pulmonary trunks of the developing heart (Fig. 3M-T and data not shown). Similar β-gal activity was observed in control and Foxm1 mutant embryos (Fig. 3M-T). Thus, Foxm1 deletion from smooth muscle cells does not alter canonical Wnt signaling during embryogenesis.

Foxm1 does not influence differentiation of smooth muscle cells

Recent studies demonstrated that Foxm1 regulates differentiation of hepatoblasts, endothelial cells and neural precursor cells in mouse and *Xenopus* embryos (Krupczak-Hollis et al., 2004; Kim et al., 2005a; Ueno et al., 2008). To determine the role of Foxm1 in differentiation of smooth muscle cells, we used *smFoxm1*$^{-/-}$ embryos to examine expression of smooth muscle marker proteins at E18.5. *smFoxm1*$^{-/-}$ and control *Foxm1*$^{fl/fl}$ embryos displayed similar expression of both the early (α-smooth muscle actin, α-SM and smooth muscle myosin heavy chain, smMHC) and the late markers of smooth muscle cells (γ-smooth muscle actin, γ-SM

and smooth muscle-specific calponin, smCalponin) in embryonic blood vessels and pulmonary airways (Fig. 4A). Furthermore, *smFoxm1*$^{-/-}$ and control *Foxm1*$^{fl/fl}$ esophagi displayed similar expression pattern for both α-SM and γ-SM, both of which were detected in three esophageal layers: an inner submucosal layer directly adjacent to the epithelium, and two smooth muscle layers representing longitudinal and circumferential layers (Fig. 4B). Expression of epithelial-specific marker Foxa2 and endothelial-specific marker Pecam-1 was not changed in *smFoxm1*$^{-/-}$ esophagus and artery, respectively (Fig. 4A-B). These results suggest that Foxm1 deficiency does not influence the differentiation of smooth muscle cells during embryonic development.

During embryogenesis, skeletal muscle contributes to the development of esophageal smooth muscle layers (Kablar et al., 2000; Rishniw et al., 2003). To determine whether there was a normal contribution of skeletal muscle to *smFoxm1*$^{-/-}$ esophagus, E18.5 embryos were stained for the presence of skeletal muscle cells using an antibody to the skeletal-muscle specific transcription factor MyoD. Although *smFoxm1*$^{-/-}$ esophagi contained less MyoD-positive cells compared to control *Foxm1*$^{fl/fl}$ embryos (Fig. 4B), no significant differences were observed in percentages of MyoD-positive cells among total numbers of muscle cells in the developing esophagus (data not shown). Thus, Foxm1 deficiency does not influence differentiation of skeletal muscle in *smFoxm1*$^{-/-}$ esophagus.

Diminished smooth muscle proliferation in *smFoxm1*$^{-/-}$ embryos

Immunohistochemistry was used to compare cellular proliferation and apoptosis in *smFoxm1*$^{-/-}$ and control *Foxm1*$^{fl/fl}$ embryos. Rare apoptosis was observed in newborn *Foxm1*$^{fl/fl}$ mice as demonstrated by immunostaining with an antibody specific to activated form of caspase 3 (Fig. 5A). In contrast, *smFoxm1*$^{-/-}$ newborn mice displayed an increased apoptosis in the lung (Fig. 5B-C), pulmonary blood vessels (Fig. 5E-F) and esophagus (Fig. 5H-I). Apoptosis was observed in both myocytes (Fig. 5H) and other cell types directly adjacent to muscle layers (Fig. 5F and I). Total numbers of caspase 3 positive cells were significantly increased in the lung of *smFoxm1*$^{-/-}$ mice when compared to either *Foxm1*$^{fl/fl}$ or *smMHC-Cre-GFP*$^{tg/-}$ lungs (Fig. 5J-L).

Cellular proliferation in *smFoxm1*$^{-/-}$ embryos was assessed by immunostaning using antibody against the cell proliferation marker Ki-67. In control *Foxm1*$^{fl/fl}$ and *smMHC-Cre-GFP*$^{tg/-}$ embryos, Ki-67 positive cells were readily detected in endothelial and smooth muscle layers of the developing aorta, as well as in all layers of the developing esophagus (Fig. 6A). Although cellular proliferation in epithelial cells was normal, diminished Ki-67 staining was observed in smooth muscle cells of *smFoxm1*$^{-/-}$ embryos (Fig. 6A-B). In comparison to control embryos, total numbers of Ki-67 positive smooth muscle cells were significantly decreased in *smFoxm1*$^{-/-}$ blood vessels and esophagi (Fig. 6C). These results demonstrated that Foxm1 deficiency reduces cellular proliferation in developing smooth muscle cells.

Foxm1 depletion causes decreased progression into mitosis in smooth muscle cells *in vitro*

In order to determine whether Foxm1 directly induces proliferation of smooth muscle cells *in vitro*, human aortic vascular smooth muscle cells (HAVSMC) were transfected with short interfering RNA (siRNA) duplex specific to the human Foxm1 mRNA (siFoxm1) or with mutant siFoxm1 duplex (mutFoxm1) containing five mutations in the siRNA structure (Wang et al., 2005a; Kim et al., 2006). Seventy-two hours later, cells were stained with propidium iodide (PI) and examined for DNA content by flow cytometry analysis. Foxm1-depletion in HAVSMC cells caused a significant reduction in G0/G1-phase cells and a decrease in mitotic progression as evidenced by a 2-fold increase in G2/M-phase (4N DNA content) with accumulation of polyploid cells (Fig. 6D). To distinguish between G2 and M phases of the cell cycle and to visualize cells undergoing mitosis, siRNA-transfected cells were subjected to

immunostaining with antibody specific to phospho-Histone H3 (PH3), a marker for mitotic cells. Depletion of Foxm1 caused a 75% reduction in the number of PH3-positive HAVSMC cells compared to either untransfected HAVSMC cells or cells transfected with mutFoxm1 (Fig. 6E). These results suggest that depletion of Foxm1 in cultured smooth muscle cells caused a G2 arrest with accumulation of polyploid cells due to a significant decrease in mitotic progression.

Gene expression profile in *Foxm1*-deficient smooth muscle cells

In order to identify potential Foxm1-target genes in smooth muscle cells, we performed analysis of mouse Affymetrix microarrays that were hybridized with cDNA probes synthesized from either siFoxm1-transfected or mock-transfected HAVSMC cells. This analysis identified 448 genes in which expression was either significantly decreased (> 2.0-fold, 421 genes) or increased (> 2.0-fold, 27 genes) after the Foxm1-depletion (see GEO database for a complete list of genes with altered expression levels in siFoxm1-transfected HAVSMC cells; http://www.ncbi.nlm.nih.gov/geo/query/acc.cgi?acc=GSE17543; accession # GSE17543). Differentially expressed genes in siFoxm1-transfected HAVSMC cells were functionally classified according to Gene Ontology (GO). Gene Ontology analysis was performed using David (database for annotation, visualization, and integrated discovery) (Dennis et al., 2003). “Mitosis” was the most significantly over-represented process, which accounted for 22% of down-regulated genes with a Fisher Exact Test P-Value of 1.54E-37 (Table 3). “Negative regulation of cellular processes “ and “negative regulation of apoptosis” were significantly enriched in subset of up-regulated genes (Table 3). In Table 4, we summarized our focus on several known Foxm1 target genes as well as novel genes regulated directly or indirectly by the Foxm1 protein.

Consistent with an efficient Foxm1 knockdown, a 10-fold reduction in Foxm1 mRNA levels was observed in siFoxm1-transfected HAVSMC cells (Table 4). A subset of mRNAs, whose expression was decreased in Foxm1-depleted cells, included centromere proteins A and F, cyclin B1, aurora B kinase, polo-like kinases (Plk) 1 and 4, JNK1 and cyclin-dependent kinase 1 (cdk1). Since these genes regulate G2/M transition of the cell cycle and are required for cytokinesis (Glover et al., 1998;Adams et al., 2001;Wang et al., 2008), their diminished levels can contribute to the cell cycle defects seen in Foxm1-depleted HAVSMC cells. Interestingly, numerous genes essential for G1/S transition were also decreased in siFoxm1-transfected HAVSMC cells (Table 4). These include cyclins A2, D1 and E2, c-Myc transcription factor, cdk2-inhibitor 3, and S-phase kinase-associated protein 2 (Skp2), the latter of which is a specificity subunit of the Skp1-Cullin 1- F-box (SCF) ubiquitin ligase complex that targets both p21 (Cip1) and p27 (Kip1) Cdk2 inhibitors for degradation during G1/S transition (Kossatz et al., 2004). Significantly decreased mRNA levels of IAP repeat-containing survivin protein, a known transcriptional target of Foxm1 (Gusarova et al., 2007), were found in siFoxm1-transfected cells (Table 4). We also found several new genes, expression of which was altered in siFoxm1-transfected HAVSMC cells. These include calmodulin 1, retinoic acid receptor α, interferon receptor 1, collagen type I receptor, placental growth factor, ADAM 10 protein, and other genes required for extracellular and intracellular signaling (Table 4). Altogether, these results suggest that Foxm1 directly or indirectly regulates expression of numerous cell cycle regulators, receptors, enzymes and adaptor proteins.

In order to verify gene expression levels in siFoxm1-transfected HAVSMC cells, quantitative real-time RT-PCR (qRT-PCR) was performed using primers specific to several Foxm1 target genes (Table 1). Approximately 10-fold reduction in Foxm1 mRNA levels was observed in siFoxm1-transfected HAVSMC cells when compared to either untransfected cells or HAVSMC cells transfected with mutant siRNA (Fig. 7A). Consistent with Affymetrix microarray analysis (Table 4), Foxm1 depletion significantly decreased mRNA levels of cyclin

B1, cyclin D1, Plk1, JNK1, and cMyc (Fig. 7A). Interestingly, decreased expression of the same genes was found in G0/ G1 population of HAVSMC cells isolated by flow cytometry-based cell sorting (Fig. 7A), indicating that Foxm1 regulates expression of these genes prior to DNA replication. In G2/ M population of sorted HAVSMC cells, Foxm1 depletion was associated with decreased mRNAs of cyclin B1, Plk1 and JNK1, whereas expression of cyclin D1 and cMyc was not significantly changed (Fig.7A). Interestingly, Foxm1 depletion did not induce apoptosis in the cultured HAVSMC cells (data not shown).

Finally, to determine whether Foxm1 regulates expression of the same cell cycle regulatory genes *in vivo*, we used a laser capture microdissection of frozen E16.5 sections to isolate total RNA from developing aortas of *smFoxm1*$^{-/-}$ and control *Foxm1*$^{fl/fl}$ embryos (Fig. 7B). Expression levels of the same cell cycle regulatory genes were determined by qRT-PCR analysis. While these RNA samples contained contributions from both the muscle and non-muscle cells (endothelium, pericytes and fibroblasts), mRNA levels of Foxm1 were significantly decreased in *smFoxm1*$^{-/-}$ aortas (Fig. 7C). While cyclin D1 mRNA was not changed in *smFoxm1*$^{-/-}$ aortas, mRNAs of cyclin B1, JNK1, cMyc and M-phase promoting Cdc25B phosphatase were significantly decreased (Fig. 7C), indicating that Foxm1 induces expression of the cell cycle regulatory genes *in vivo*. Taken together, these data suggest that Foxm1 depletion inhibits cellular regulatory pathways that stimulate smooth muscle cell proliferation during embryonic vascular development.

DISCUSSION

The requirement for Foxm1 activity in smooth muscle cells was examined in *smFoxm1*$^{-/-}$ mice that contain a smooth muscle-specific deletion of exons 4 through 7, encoding the Foxm1 DNA binding domain and C-terminal transcriptional activation domains, both of which are essential for Foxm1 transcriptional activity (Krupczak-Hollis et al., 2004). Most of the *smFoxm1*$^{-/-}$ mice exhibited a perinatal lethality within the first 24 hours after birth because of severe pulmonary hemorrhage, and structural defects in arterial wall and esophagus. Although Foxm1 deletion did not influence differentiation of smooth muscle cells, decreased proliferation of smooth muscle cells was found in *smFoxm1*$^{-/-}$ blood vessels and esophagus. Proliferation defects in *smFoxm1*$^{-/-}$ embryos were associated with decreased expression of M-phase promoting Cdc25B phosphatase and cyclin B1. Progression into mitosis requires the activation of Cdk1 through assembly with cyclin B1 regulatory subunit and the removal of Cdk1 inhibitory phosphates at Thr 14 and Tyr 15 by the Cdc25B and Cdc25C phosphatases (Borgne and Meijer, 1996; Wells et al., 1999; Nilsson and Hoffmann, 2000). Therefore, diminished levels of Cdc25B and decreased levels of cyclin B1 can decrease Cdk1 activation and M-phase progression causing delayed entry into mitosis in Foxm1-deficient smooth muscle cells. These results are consistent with previous studies that reported a direct transcriptional activation of these genes by Foxm1 in cultured mouse embryonic fibroblasts (MEFs) and U2OS human osteosarcoma cell line (Wang et al., 2005a).

Our studies demonstrated that several genes critical for G1/S transition were decreased in Foxm1-deficient smooth muscle cells *in vivo* and *in vitro*. These include JNK1, c-Myc transcription factor and cyclins A2, D1 and E2 that activate Cdk proteins during G1/S transition. Cdk2 complexes with either Cyclin E or Cyclin A cooperate with Cyclin D-Cdk4/6 to phosphorylate the Retinoblastoma (RB) protein, which releases bound E2F transcription factor and allows it to stimulate expression of genes required for DNA replication (Harbour and Dean, 2000; Ishida et al., 2001). Therefore, defects in cell proliferation in *smFoxm1*$^{-/-}$ smooth muscle cells may be a direct consequence of reduced Cdk2 and Cdk4 activity causing diminished DNA replication. Our results are consistent with previously published data demonstrating that transgenic over-expression of Foxm1 in Rosa26-Foxm1 transgenic mice is

associated with premature DNA replication in pulmonary smooth muscle cells following Butylated Hydroxytoluene (BHT) lung injury (Kalinichenko et al., 2003).

In our previous studies, we generated mice with global deletion of the Foxm1 gene (homozygous for *Foxm1* null allele or *Foxm1*$^{-/-}$ mice) and demonstrated that these mice displayed an embryonic lethal phenotype between E13.5 and E16.5 (Krupczak-Hollis et al., 2004; Kim et al., 2005a; Ramakrishna et al., 2007). *Foxm1*$^{-/-}$ embryos displayed multiple abnormalities in development of embryonic heart, liver, lung and blood vessels as well as differentiation defects in capillary endothelial cells (Kim et al., 2005a) and bile duct epithelial cells (Krupczak-Hollis et al., 2004). However, since *Foxm1* is required for normal development of distinct *Foxm1*$^{-/-}$ cell lineages, these studies did not clarify specific requirements for Foxm1 activity in smooth muscle cells. Furthermore, severe ventricular hypoplasia in *Foxm1*$^{-/-}$ embryos may cause a diminished circulatory output and altered signaling, causing secondary defects in developing blood vessels. In this study, we demonstrated that Foxm1-deletion from *smFoxm1*$^{-/-}$ smooth muscle cells is sufficient to disrupt vascular development in the absence of structural heart abnormalities. Therefore, Foxm1 promotes embryonic vascular development by directly influencing proliferation of developing smooth muscle cells. Interestingly, although increased apoptosis was observed in *smFoxm1*$^{-/-}$ newborn mice, the apoptosis was not significantly increased in *smFoxm1*$^{-/-}$ embryos prior to birth. These results raise a possibility that the apoptotic phenotype in *smFoxm1*$^{-/-}$ mice was an indirect consequence of Foxm1 deficiency. Furthermore, a specific Foxm1 depletion by siRNA did not cause apoptosis in cultured smooth muscle cells, providing further support for this concept.

In contrast to structural defects in *smFoxm1*$^{-/-}$ blood vessels, no structural abnormalities were found in the developing airways, stomach or intestine of the *smFoxm1*$^{-/-}$ embryos. These results are surprising and suggest different requirements in Foxm1 function in different populations of developing smooth muscle cells. Published studies demonstrated that vascular and visceral smooth muscle cells (intestinal, esophageal and peribronchial muscle) use distinct transcription factor complexes to activate smooth muscle-specific gene promoters. Differential deletion of the serum response factor (SRF) binding sites (CArG boxes) revealed fundamental differences in importance of particular SRF-binding regions between smooth muscle subtypes (Manabe and Owens, 2001). It was also demonstrated that promoter of CRP-1 gene contains a CArG box-dependent enhancer, which directs expression in arterial but not venous or visceral smooth muscle cells (Lilly et al., 2001). Expression of GATA-5 and Foxf1 transcription factors was found to be restricted to visceral smooth muscle cells with little or no expression in vascular smooth muscle tissues (Morrisey et al., 1997; Kalinichenko et al., 2001). Selective smooth muscle defects in *smFoxm1*$^{-/-}$ embryos indicate that Foxm1 may regulate distinct genes in different subsets of smooth muscle cells. However, molecular mechanisms underlying this selectivity remain unknown. Alternatively, it is possible that Foxm1-deletion does not efficiently occur in all smooth muscle tissues during embryogenesis. While Cre recombinase protein was detected in inner circumferential muscle layers of the developing stomach and intestine, no Cre staining was observed in outer longitudinal layers of *smFoxm1*$^{-/-}$ intestine until E18.5. In contrast, *smFoxm1*$^{-/-}$ esophagi contained Cre protein in both inner and outer smooth muscle layers. Interestingly, approximately 13% of *smFoxm1*$^{-/-}$ mice survived after birth and developed a megacolon by 4 weeks of age (data not shown). Since a histological structure of the intestine in these adult *smFoxm1*$^{-/-}$ mice was normal (data not shown), the megacolon may be a result of diminished muscular tone and/or intestinal contractility in these Foxm1 mutant mice.

In summary, *smFoxm1*$^{-/-}$ mice died immediately after birth due to severe pulmonary hemorrhage, structural defects in arterial wall, and esophageal abnormalities. Although Foxm1 deletion did not influence differentiation of smooth muscle cells, decreased cellular proliferation was observed in muscle layers of embryonic blood vessels and esophagus.

Depletion of Foxm1 *in vitro* and *in vivo* was associated with reduced expression of genes required for cell cycle progression. The identification of critical regulators of myocyte proliferation, such as Foxm1, may provide novel strategies for diagnosis and treatment of congenital vascular and esophageal abnormalities.

Acknowledgments

We thank Dr. J. Whitsett for critically reviewing the manuscript. This work was supported by grants from National Institute of Health (HL 84151-01) and March of Dimes Birth Defects Foundation (6-FY2005-325).

REFERENCES

Ackermann Misfeldt A, Costa RH, Gannon M. Beta-cell proliferation, but not neogenesis, following 60% partial pancreatectomy is impaired in the absence of FoxM1. Diabetes 2008;57:3069–3077. [PubMed: 18728229]

Adams RR, Carmena M, Earnshaw WC. Chromosomal passengers and the (aurora) ABCs of mitosis. Trends Cell Biol 2001;11:49–54. [PubMed: 11166196]

Belaguli NS, Sepulveda JL, Nigam V, Charron F, Nemer M, Schwartz RJ. Cardiac tissue enriched factors serum response factor and GATA-4 are mutual coregulators. Mol Cell Biol 2000;20:7550–7558. [PubMed: 11003651]

Borgne A, Meijer L. Sequential dephosphorylation of p34(cdc2) on Thr-14 and Tyr-15 at the prophase/metaphase transition. J. Biol. Chem 1996;271:27847–27854. [PubMed: 8910383]

Camoretti-Mercado B, Dulin NO, Solway J. Serum response factor function and dysfunction in smooth muscle. Respir Physiol Neurobiol 2003;137:223–235. [PubMed: 14516728]

Carmeliet P, Ferreira V, Breier G, Pollefeyt S, Kieckens L, Gertsenstein M, Fahrig M, Vandenhoeck A, Harpal K, Eberhardt C, Declercq C, Pawling J, Moons L, Collen D, Risau W, Nagy A. Abnormal blood vessel development and lethality in embryos lacking a single VEGF allele. Nature 1996;380:435–439. [PubMed: 8602241]

Chi JT, Rodriguez EH, Wang Z, Nuyten DS, Mukherjee S, van de Rijn M, van de Vijver MJ, Hastie T, Brown PO. Gene expression programs of human smooth muscle cells: tissue-specific differentiation and prognostic significance in breast cancers. PLoS Genet 2007;3:1770–1784. [PubMed: 17907811]

Clark KL, Halay ED, Lai E, Burley SK. Co-crystal structure of the HNF-3/fork head DNA-recognition motif resembles histone H5. Nature 1993;364:412–420. [PubMed: 8332212]

Clevidence DE, Overdier DG, Tao W, Qian X, Pani L, Lai E, Costa RH. Identification of nine tissue-specific transcription factors of the hepatocyte nuclear factor 3/forkhead DNA-binding-domain family. Proc. Natl. Acad. Sci. USA 1993;90:3948–3952. [PubMed: 7683413]

Dave V, Childs T, Xu Y, Ikegami M, Besnard V, Maeda Y, Wert SE, Neilson JR, Crabtree GR, Whitsett JA. Calcineurin/Nfat signaling is required for perinatal lung maturation and function. J Clin Invest 2006;116:2597–2609. [PubMed: 16998587]

Dennis G Jr. Sherman BT, Hosack DA, Yang J, Gao W, Lane HC, Lempicki RA. DAVID: Database for Annotation, Visualization, and Integrated Discovery. Genome Biol 2003;4:P3. [PubMed: 12734009]

Gittenberger-de Groot AC, DeRuiter MC, Bergwerff M, Poelmann RE. Smooth muscle cell origin and its relation to heterogeneity in development and disease. Arterioscler Thromb Vasc Biol 1999;19:1589–1594. [PubMed: 10397674]

Glover DM, Hagan IM, Tavares AA. Polo-like kinases: a team that plays throughout mitosis. Genes Dev 1998;12:3777–3787. [PubMed: 9869630]

Gusarova GA, Wang IC, Major ML, Kalinichenko VV, Ackerson T, Petrovic V, Costa RH. A cell-penetrating ARF peptide inhibitor of FoxM1 in mouse hepatocellular carcinoma treatment. J Clin Invest 2007;117:99–111. [PubMed: 17173139]

Halayko AJ, Solway J. Molecular mechanisms of phenotypic plasticity in smooth muscle cells. J Appl Physiol 2001;90:358–368. [PubMed: 11133929]

Hao H, Gabbiani G, Bochaton-Piallat ML. Arterial smooth muscle cell heterogeneity: implications for atherosclerosis and restenosis development. Arterioscler Thromb Vasc Biol 2003;23:1510–1520. [PubMed: 12907463]

Harbour JW, Dean DC. The Rb/E2F pathway: expanding roles and emerging paradigms. Genes Dev 2000;14:2393–2409. [PubMed: 11018009]

Ishida S, Huang E, Zuzan H, Spang R, Leone G, West M, Nevins JR. Role for E2F in control of both DNA replication and mitotic functions as revealed from DNA microarray analysis. Mol Cell Biol 2001;21:4684–4699. [PubMed: 11416145]

Itaranta P, Chi L, Seppanen T, Niku M, Tuukkanen J, Peltoketo H, Vainio S. Wnt-4 signaling is involved in the control of smooth muscle cell fate via Bmp-4 in the medullary stroma of the developing kidney. Dev Biol 2006;293:473–483. [PubMed: 16546160]

Kablar B, Tajbakhsh S, Rudnicki MA. Transdifferentiation of esophageal smooth to skeletal muscle is myogenic bHLH factor-dependent. Development 2000;127:1627–1639. [PubMed: 10725239]

Kaestner KH, Lee KH, Schlondorff J, Hiemisch H, Monaghan AP, Schutz G. Six members of the mouse forkhead gene family are developmentally regulated. Proc. Natl. Acad. Sci. USA 1993;90:7628–7631. [PubMed: 7689224]

Kalin TV, Wang IC, Ackerson TJ, Major ML, Detrisac CJ, Kalinichenko VV, Lyubimov A, Costa RH. Increased levels of the FoxM1 transcription factor accelerate development and progression of prostate carcinomas in both TRAMP and LADY transgenic mice. Cancer Res 2006;66:1712–1720. [PubMed: 16452231]

Kalin TV, Wang IC, Meliton L, Zhang Y, Wert SE, Ren X, Snyder J, Bell SM, Graf L Jr. Whitsett JA, Kalinichenko VV. Forkhead Box m1 transcription factor is required for perinatal lung function. Proc Natl Acad Sci U S A 2008;105:19330–19335. [PubMed: 19033457]

Kalinichenko VV, Gusarova GA, Tan Y, Wang IC, Major ML, Wang X, Yoder HM, Costa RH. Ubiquitous expression of the forkhead box M1B transgene accelerates proliferation of distinct pulmonary cell-types following lung injury. J Biol Chem 2003;278:37888–37894. [PubMed: 12867420]

Kalinichenko VV, Lim L, Beer-Stoltz D, Shin B, Rausa FM, Clark J, Whitsett JA, Watkins SC, Costa RH. Defects in Pulmonary Vasculature and Perinatal Lung Hemorrhage in Mice Heterozygous Null for the Forkhead Box f1 transcription factor. Dev Biol 2001;235:489–506. [PubMed: 11437453]

Kalinichenko VV, Major M, Wang X, Petrovic V, Kuechle J, Yoder HM, Shin B, Datta A, Raychaudhuri P, Costa RH. Forkhead Box m1b Transcription Factor is Essential for Development of Hepatocellular Carcinomas and is Negatively Regulated by the p19ARF Tumor Suppressor. Genes & Development 2004;18:830–850. [PubMed: 15082532]

Katoh Y, Molkentin JD, Dave V, Olson EN, Periasamy M. MEF2B is a component of a smooth muscle-specific complex that binds an A/T-rich element important for smooth muscle myosin heavy chain gene expression. J Biol Chem 1998;273:1511–1518. [PubMed: 9430690]

Kim IM, Ackerson T, Ramakrishna S, Tretiakova M, Wang IC, Kalin TV, Major ML, Gusarova GA, Yoder HM, Costa RH, Kalinichenko VV. The Forkhead Box m1 Transcription Factor Stimulates the Proliferation of Tumor Cells during Development of Lung Cancer. Cancer Res 2006;66:2153–2161. [PubMed: 16489016]

Kim IM, Ramakrishna S, Gusarova GA, Yoder HM, Costa RH, Kalinichenko VV. The forkhead box M1 transcription factor is essential for embryonic development of pulmonary vasculature. J Biol Chem 2005a;280:22278–22286. [PubMed: 15817462]

Kim IM, Zhou Y, Ramakrishna S, Hughes DE, Solway J, Costa RH, Kalinichenko VV. Functional characterization of evolutionary conserved DNA regions in forkhead box f1 gene locus. J Biol Chem 2005b;280:37908–37916. [PubMed: 16144835]

Korver W, Roose J, Clevers H. The winged-helix transcription factor Trident is expressed in cycling cells. Nucleic Acids Res 1997;25:1715–1719. [PubMed: 9108152]

Korver W, Schilham MW, Moerer P, van den Hoff MJ, Dam K, Lamers WH, Medema RH, Clevers H. Uncoupling of S phase and mitosis in cardiomyocytes and hepatocytes lacking the winged-helix transcription factor trident. Curr Biol 1998;8:1327–1330. [PubMed: 9843684]

Kossatz U, Dietrich N, Zender L, Buer J, Manns MP, Malek NP. Skp2-dependent degradation of p27kip1 is essential for cell cycle progression. Genes Dev 2004;18:2602–2607. [PubMed: 15520280]

Krupczak-Hollis K, Wang X, Kalinichenko VV, Gusarova GA, Wang I-C, Dennewitz MB, Yoder HM, Kiyokawa H, Kaestner KH, Costa RH. The Mouse Forkhead Box m1 Transcription Factor is Essential

for Hepatoblast Mitosis and Development of Intrahepatic Bile Ducts and Vessels during Liver Morphogenesis. Dev Biol 2004;276:74–88. [PubMed: 15531365]

Kumar MS, Owens GK. Combinatorial control of smooth muscle-specific gene expression. Arterioscler Thromb Vasc Biol 2003;23:737–747. [PubMed: 12740224]

Lilly B, Olson EN, Beckerle MC. Identification of a CArG box-dependent enhancer within the cysteine-rich protein 1 gene that directs expression in arterial but not venous or visceral smooth muscle cells. Dev Biol 2001;240:531–547. [PubMed: 11784081]

Manabe I, Owens GK. CArG elements control smooth muscle subtype-specific expression of smooth muscle myosin in vivo. J Clin Invest 2001;107:823–834. [PubMed: 11285301]

Morrisey EE, Ip HS, Tang Z, Lu MM, Parmacek MS. GATA-5: a transcriptional activator expressed in a novel temporally and spatially-restricted pattern during embryonic development. Dev Biol 1997;183:21–36. [PubMed: 9119112]

Nilsson I, Hoffmann I. Cell cycle regulation by the Cdc25 phosphatase family. Prog Cell Cycle Res 2000;4:107–114. [PubMed: 10740819]

Pan D, Zhe X, Jakkaraju S, Taylor GA, Schuger L. P311 induces a TGF-beta1-independent, nonfibrogenic myofibroblast phenotype. J Clin Invest 2002;110:1349–1358. [PubMed: 12417574]

Pipes GC, Creemers EE, Olson EN. The myocardin family of transcriptional coactivators: versatile regulators of cell growth, migration, and myogenesis. Genes Dev 2006;20:1545–1556. [PubMed: 16778073]

Ramakrishna S, Kim IM, Petrovic V, Malin D, Wang IC, Kalin TV, Meliton L, Zhao YY, Ackerson T, Qin Y, Malik AB, Costa RH, Kalinichenko VV. Myocardium defects and ventricular hypoplasia in mice homozygous null for the Forkhead Box M1 transcription factor. Dev Dyn 2007;236:1000–1013. [PubMed: 17366632]

Rishniw M, Xin HB, Deng KY, Kotlikoff MI. Skeletal myogenesis in the mouse esophagus does not occur through transdifferentiation. Genesis 2003;36:81–82. [PubMed: 12820168]

Rossant J, Howard L. Signaling pathways in vascular development. Annu Rev Cell Dev Biol 2002;18:541–573. [PubMed: 12142271]

Saint-Jeannet JP, Levi G, Girault JM, Koteliansky V, Thiery JP. Ventrolateral regionalization of Xenopus laevis mesoderm is characterized by the expression of alpha-smooth muscle actin. Development 1992;115:1165–1173. [PubMed: 1451663]

Shu W, Jiang YQ, Lu MM, Morrisey EE. Wnt7b regulates mesenchymal proliferation and vascular development in the lung. Development 2002;129:4831–4842. [PubMed: 12361974]

Thayer JM, Meyers K, Giachelli CM, Schwartz SM. Formation of the arterial media during vascular development. Cell Mol Biol Res 1995;41:251–262. [PubMed: 8775983]

Ueno H, Nakajo N, Watanabe M, Isoda M, Sagata N. FoxM1-driven cell division is required for neuronal differentiation in early Xenopus embryos. Development 2008;135:2023–2030. [PubMed: 18469223]

Wang D, Chang PS, Wang Z, Sutherland L, Richardson JA, Small E, Krieg PA, Olson EN. Activation of cardiac gene expression by myocardin, a transcriptional cofactor for serum response factor. Cell 2001;105:851–862. [PubMed: 11439182]

Wang IC, Chen YJ, Hughes D, Petrovic V, Major ML, Park HJ, Tan Y, Ackerson T, Costa RH. Forkhead box M1 regulates the transcriptional network of genes essential for mitotic progression and genes encoding the SCF (Skp2-Cks1) ubiquitin ligase. Mol Cell Biol 2005a;25:10875–10894. [PubMed: 16314512]

Wang IC, Chen YJ, Hughes DE, Ackerson T, Major ML, Kalinichenko VV, Costa RH, Raychaudhuri P, Tyner AL, Lau LF. FOXM1 regulates transcription of JNK1 to promote the G1/S transition and tumor cell invasiveness. J Biol Chem 2008;283:20770–20778. [PubMed: 18524773]

Wang Z, Shu W, Lu MM, Morrisey EE. Wnt7b activates canonical signaling in epithelial and vascular smooth muscle cells through interactions with Fzd1, Fzd10, and LRP5. Mol Cell Biol 2005b; 25:5022–5030. [PubMed: 15923619]

Watanabe M, Layne MD, Hsieh CM, Maemura K, Gray S, Lee ME, Jain MK. Regulation of smooth muscle cell differentiation by AT-rich interaction domain transcription factors Mrf2alpha and Mrf2beta. Circ Res 2002;91:382–389. [PubMed: 12215486]

Wells NJ, Watanabe N, Tokusumi T, Jiang W, Verdecia MA, Hunter T. The C-terminal domain of the Cdc2 inhibitory kinase Myt1 interacts with Cdc2 complexes and is required for inhibition of G(2)/M progression. J Cell Sci 1999;112:3361–3371. [PubMed: 10504341]

Xin HB, Deng KY, Rishniw M, Ji G, Kotlikoff MI. Smooth muscle expression of Cre recombinase and eGFP in transgenic mice. Physiol Genomics 2002;10:211–215. [PubMed: 12209023]

Ye H, Kelly TF, Samadani U, Lim L, Rubio S, Overdier DG, Roebuck KA, Costa RH. Hepatocyte nuclear factor 3/fork head homolog 11 is expressed in proliferating epithelial and mesenchymal cells of embryonic and adult tissues. Mol Cell Biol 1997;17:1626–1641. [PubMed: 9032290]

Yoshida Y, Wang IC, Yoder HM, Davidson NO, Costa RH. The forkhead box M1 transcription factor contributes to the development and growth of mouse colorectal cancer. Gastroenterology 2007;132:1420–1431. [PubMed: 17408638]

Zhang H, Ackermann AM, Gusarova GA, Lowe D, Feng X, Kopsombut UG, Costa RH, Gannon M. The FoxM1 transcription factor is required to maintain pancreatic beta-cell mass. Mol Endocrinol 2006;20:1853–1866. [PubMed: 16556734]

Zhao YY, Gao XP, Zhao YD, Mirza MK, Frey RS, Kalinichenko VV, Wang IC, Costa RH, Malik AB. Endothelial cell-restricted disruption of FoxM1 impairs endothelial repair following LPS-induced vascular injury. J Clin Invest 2006;116:2333–2343. [PubMed: 16955137]

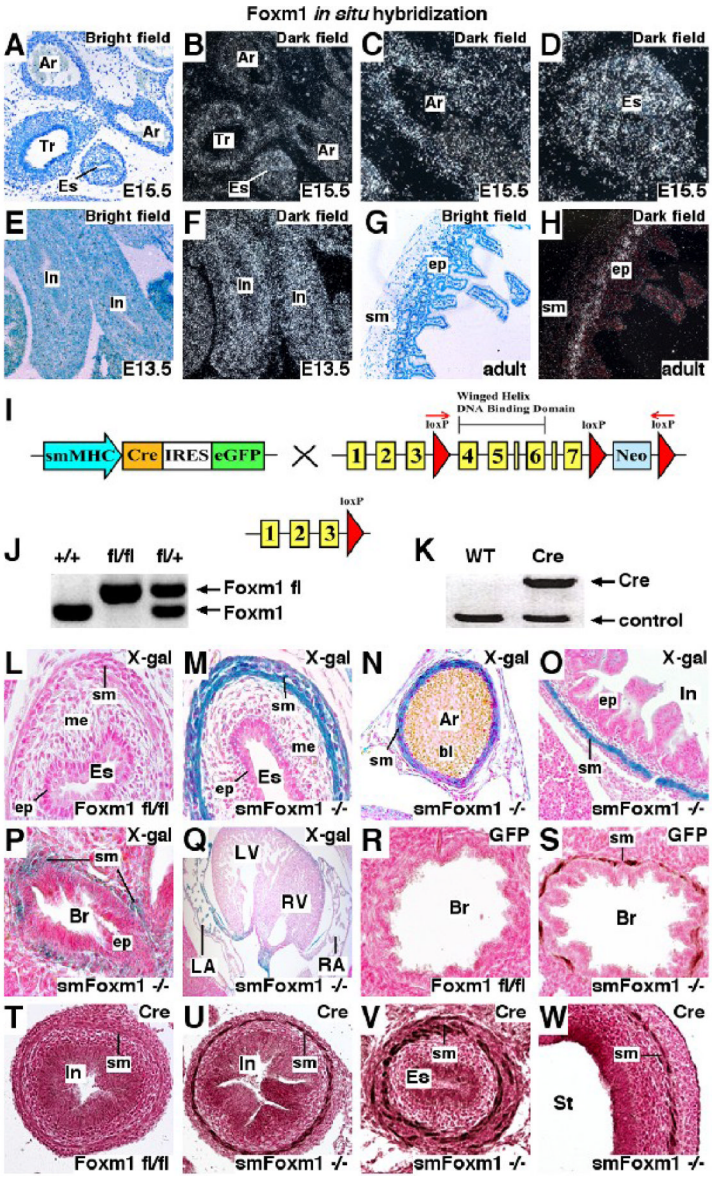

Figure 1. Deletion of Foxm1 in smooth muscle cells

A-H, Foxm1 expression in smooth muscle cells during mouse embryonic development. Paraffin sections from E13.5 embryos (E-F), E15.5 embryos (A-D) or adult mice (G-H) were used for *in situ* hybridization with ^{35}S-labeled antisense riboprobe specific to mouse Foxm1. Sections were counterstained with toluidine blue. During embryogenesis, Foxm1 is expressed in all cell types, including smooth muscle (sm) and epithelial cells (ep). Abbreviations: Ar, artery; Tr, trachea; Es, esophagus; In, intestine. In adult mice, Foxm1 expression is restricted to epithelial cells (ep) of intestinal crypts. *I*, Schematic drawing of Cre-mediated deletion in Foxm1-floxed gene. To delete Foxm1 in smooth muscle cells, *Foxm1*$^{fl/fl}$ mice were bred with *smMHC-Cre-GFP*$^{tg/-}$ mice to generate *smMHC-Cre-GFP*$^{tg/-}$ *Foxm1*$^{fl/fl}$ double transgenic mice, containing a deletion of exons 4-7 of the mouse Foxm1 gene (*smFoxm1*$^{-/-}$ mice). *J-K*, PCR analysis of genomic DNA identified Foxm1-floxed allele and *smMHC-Cre-GFP* transgene. *L-Q*, Cre recombination in smooth muscle cells of *smFoxm1*$^{-/-}$ mice. β-gal activity was observed in arteries (Ar), esophagus (Es), bronchi (Br), and intestine (In) of *smFoxm1*$^{-/-}$/ R26R E15.5 embryos. The Foxm1 mutants displayed a mosaic Cre recombination in left (LA) and right

atriums (RA) but not in left (LV) and right ventricles (RV). β-gal activity was not detected in control *Foxm1*$^{fl/fl}$/ R26R embryos. Sections were counterstained with nuclear fast red. *R-W*, Cre transgene is specifically expressed in *smFoxm1*$^{-/-}$ smooth muscle cells. Paraffin sections from *Foxm1*$^{fl/fl}$ and *smFoxm1*$^{-/-}$ E15.5 embryos were stained with either Cre antibody (T-W) or GFP antibody (R-S). Magnifications: Q, x50; A-B and E-H, x100; C-D, N-O and T-W, x200; remaining panels, x400.

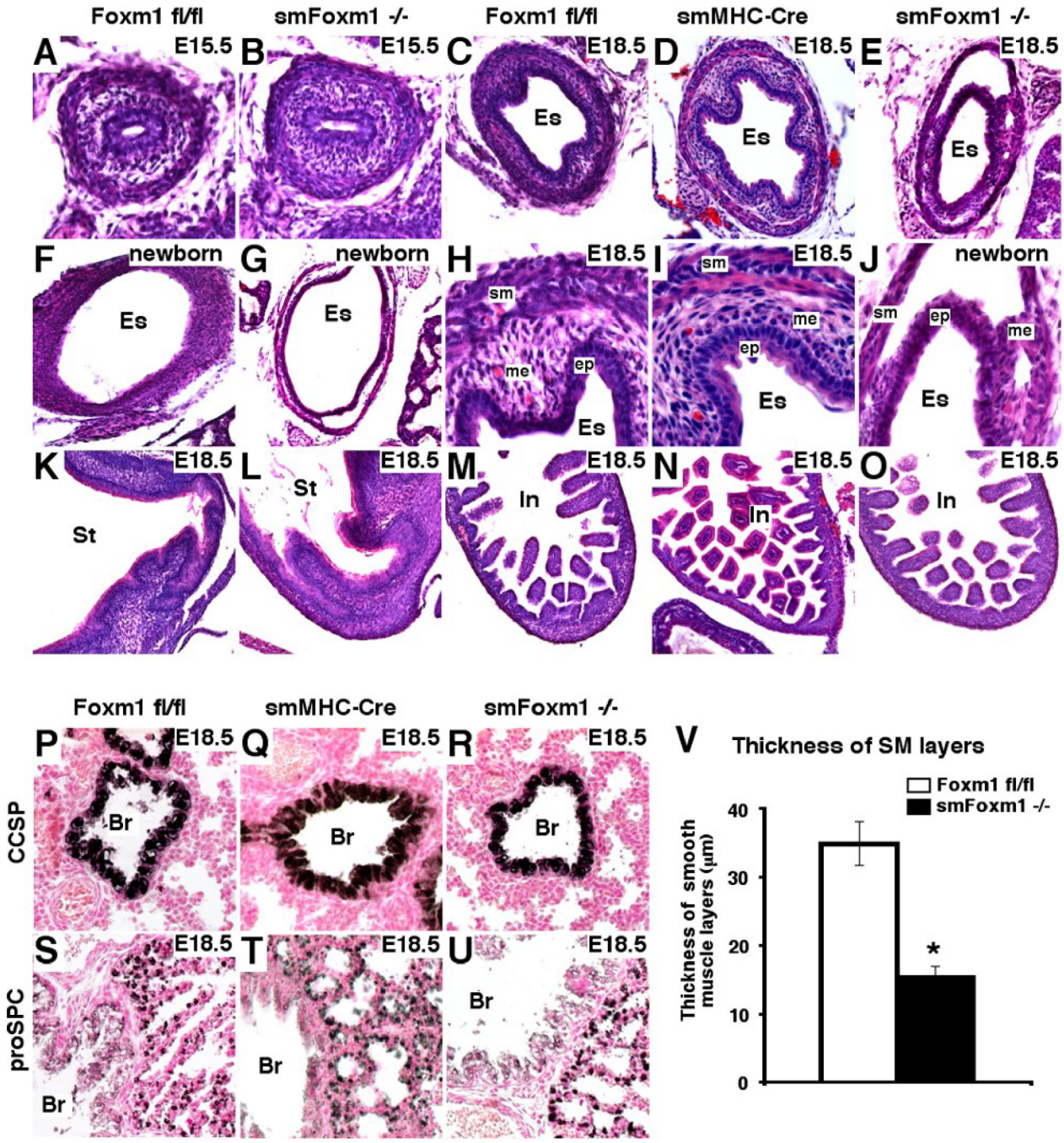

Figure 2. Esophageal defects in *smFoxm1*$^{-/-}$ mice

A-O, Esophageal defects in Foxm1-deficient mice. Paraffin sections from *smFoxm1*$^{-/-}$, *Foxm1*$^{fl/fl}$ and *smMHC-Cre-GFP*$^{tg/-}$ embryos were stained with hematoxylin and eosin (H&E). Histological structure of esophagus (Es) was similar in *smFoxm1*$^{-/-}$ and control *Foxm1*$^{fl/fl}$ littermates at E15.5 (A-B). Thinning of esophageal muscle (sm) and loss of mesenchymal cells (me) were observed in *smFoxm1*$^{-/-}$ E18.5 embryos (C-E and H-J) and newborn mice (F-G). No structural defects were observed in *smFoxm1*$^{-/-}$ stomach (K-L) and intestine (M-O). *P-U*, Normal expression of CCSP and proSPC epithelial marker proteins in Foxm1-deficient lungs. Staining was visualized using biotinylated secondary antibody, avidin-HRP, and DAB substrate (dark brown), and then counterstained with nuclear fast red. *V*,

Diminished thickness of esophageal muscle is observed in *smFoxm1*$^{-/-}$ E18.5 embryos. Means ± S.D. were determined using three different *smFoxm1*$^{-/-}$ and control *Foxm1*$^{fl/fl}$ embryos (10 random sections for each embryo). A p value < 0.05 is shown with asterisk. Abbreviations: Es, esophagus; In, intestine; St, stomach; Br, bronchiole; ep, epithelial cells. Magnification: A-B, x200; H-J and P-U, x400; remaining panels, x100.

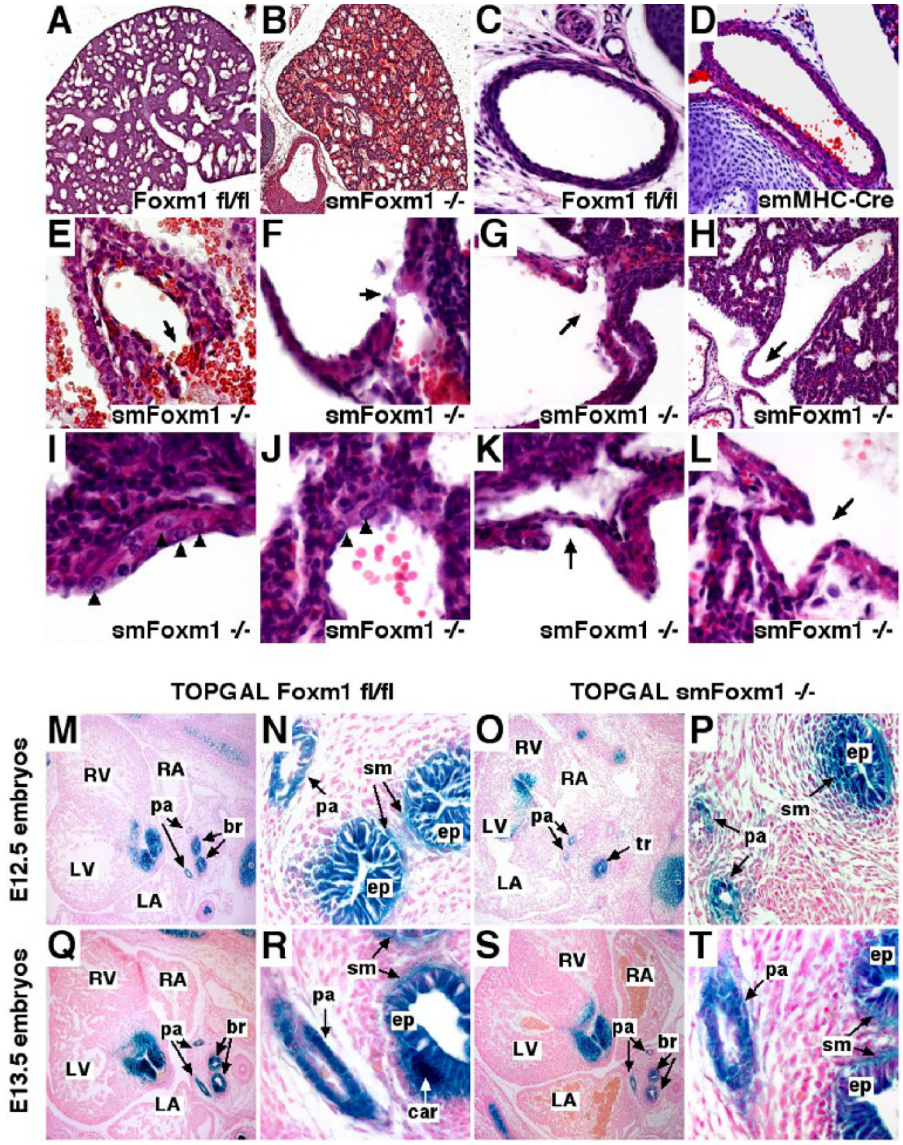

Figure 3. Perinatal pulmonary hemorrhage and vascular defects in *smFoxm1*$^{-/-}$ mice

A-L, Pulmonary hemorrhage in Foxm1-deficient mice. Embryonic lungs from *smFoxm1*$^{-/-}$, *Foxm1*$^{fl/fl}$ and *smMHC-Cre-GFP*$^{tg/-}$ mice were fixed, paraffin-embedded, sectioned, and stained with hematoxylin and eosin (H&E). *smFoxm1*$^{-/-}$ newborn mice displayed extensive pulmonary hemorrhage with red blood cells present in bronchioles and peripheral pulmonary saccules (A-B). No structural abnormalities were observed in either *Foxm1*$^{fl/fl}$ (C) or *smMHC-Cre-GFP*$^{tg/-}$ blood vessels (D). Pulmonary arteries from *smFoxm1*$^{-/-}$ mice displayed tears in arterial walls and disruption of smooth muscle layers (F, E, shown with arrows), multiple hernias (G, H, K and L), as well as accumulation of large cells with round nuclei (I, J, shown with arrowheads). *M-T*, Activity of canonical Wnt signaling pathway in *smFoxm1*$^{-/-}$ embryos. TOPGAL$^{tg/-}$/ *smFoxm1*$^{-/-}$ and control TOPGAL$^{tg/-}$/ *smFoxm1*$^{fl/fl}$ embryos were stained for β-gal activity at E12.5 (M-P) and E13.5 (Q-T). Sections were counterstained with nuclear fast red. Control and Foxm1 mutant embryos displayed similar β-gal activity (blue) in pulmonary arteries (pa), and bronchial epithelium (ep), smooth muscle (sm) and cartilage (car) of bronchi (br), as well as in aortic outflow and pulmonary trunks of the developing heart. Abbreviations:

LA, left atrium; RA, right atrium; LV, left ventricle; RV, right ventricle. Magnification: A-B, M, O, Q and S, x50; H, x100; I-L, R and T, x400; remaining panels, x200.

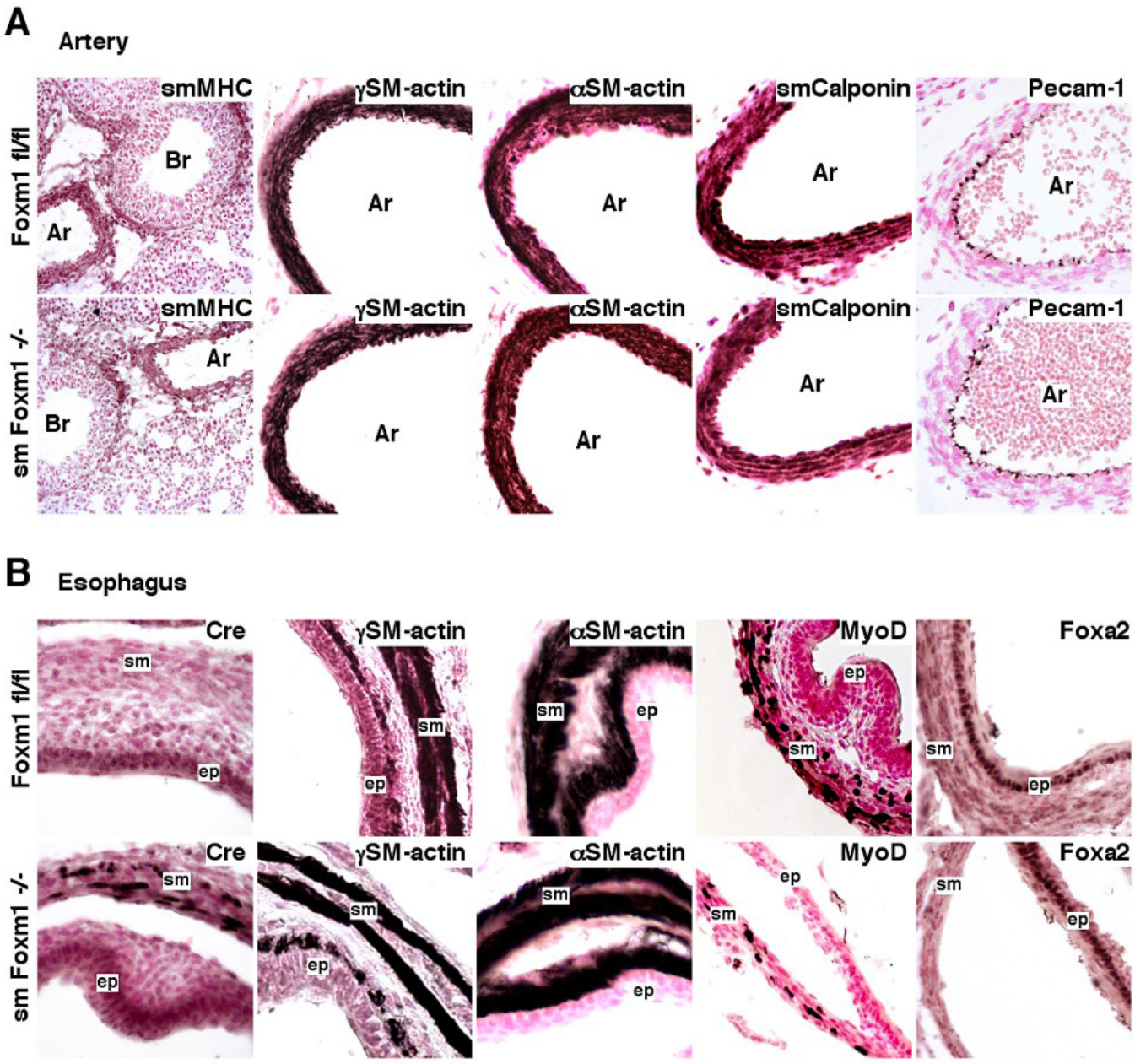

Figure 4. *smFoxm1*$^{-/-}$ embryos displayed normal expression of smooth muscle marker proteins

E18.5 sections from *smFoxm1*$^{-/-}$ and control *Foxm1*$^{fl/fl}$ embryos were stained with antibodies against smooth muscle myosin heavy chain (smMHC), α-smooth muscle actin (αSM-actin), γ-smooth muscle actin (γSM-actin), smooth muscle specific calponin (smCalponin), Cre recombinase (Cre), MyoD transcription factor, Pecam-1 and Foxa2. Staining was visualized using biotinylated secondary antibody, avidin-HRP, and DAB substrate (dark brown), and then counterstained with nuclear fast red. Similar expression of smooth marker proteins was observed in *smFoxm1*$^{-/-}$ and control *Foxm1*$^{fl/fl}$ arteries (A) and esophagi (B) Abbreviations: Ar, artery; Br, bronchiole; ep, epithelial cells; sm, smooth muscle cells. Magnifications: left panels in A, x100; remaining panels, x400.

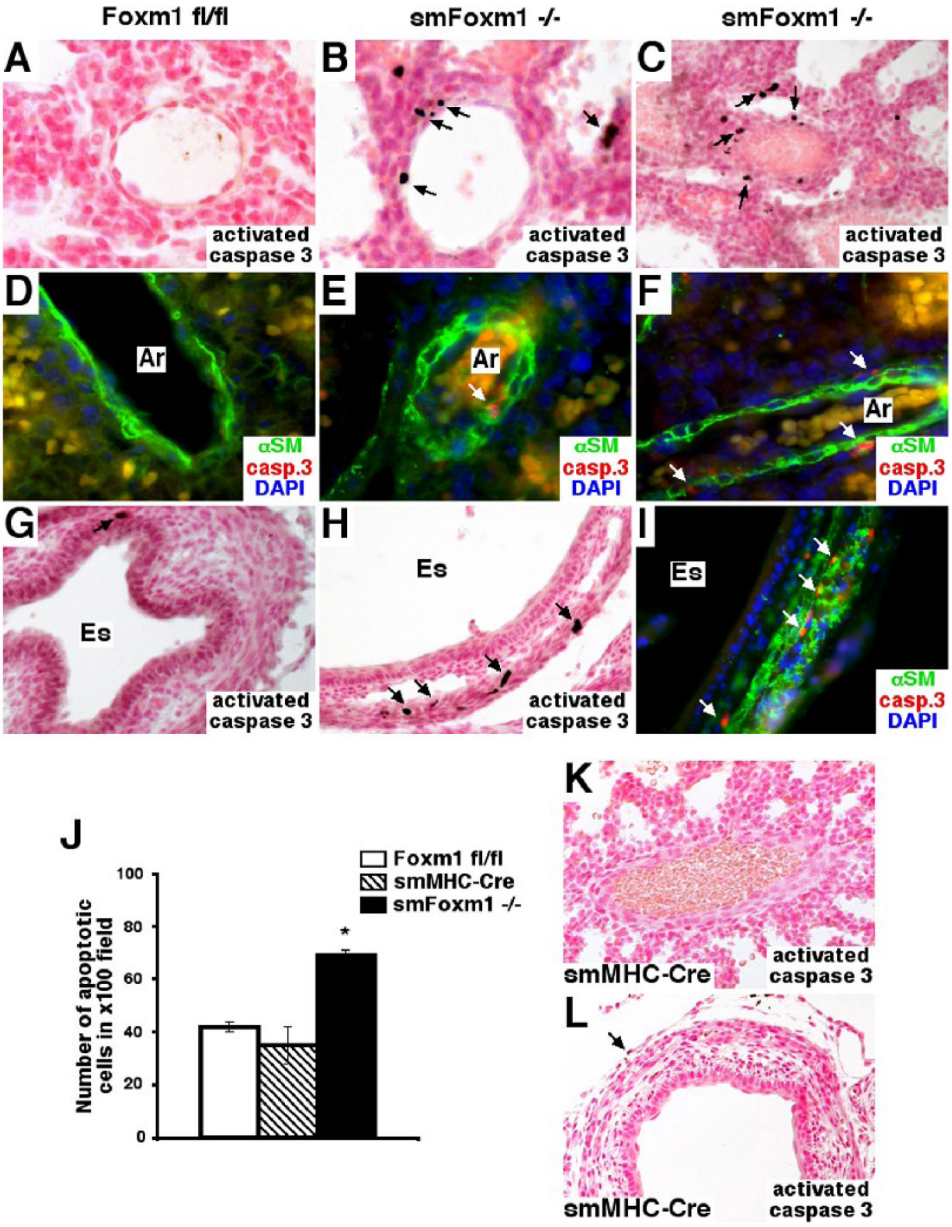

Figure 5. Increased apoptosis in newborn *smFoxm1*$^{-/-}$ mice

A-I and K-L, Increased apoptosis in *smFoxm1*$^{-/-}$ mice. Paraffin sections from newborn *smFoxm1*$^{-/-}$, *Foxm1*$^{fl/fl}$, *smMHC-Cre-GFP*$^{tg/-}$ mice were stained with antibodies against cleaved caspase 3 (dark brown, shown with arrows) and counterstained with nuclear fast red (A-C, G-H and K-L). In co-localization experiments (D-F and I), paraffin sections were stained with antibodies against cleaved caspase 3 (red fluorescence), α-SM actin antibodies (green fluorescence) and DAPI (blue fluorescence). Erythrocytes displayed yellow autofluorescence. Rare apoptosis was observed in *Foxm1*$^{fl/fl}$ esophagus (G) and blood vessels (A and D) as well as in *smMHC-Cre-GFP*$^{tg/-}$ embryos (K-L). *smFoxm1*$^{-/-}$ mice displayed an increased apoptosis in pulmonary blood vessels (B-C and E), esophagus (H), as well as cells adjacent to muscle layers (F and I, shown with arrows). Abbreviations: Ar, Artery; Es, esophagus. Magnifications: C, G-H and L, x200; remaining panels, x400. *J*, Increased number of apoptotic cells in *smFoxm1*$^{-/-}$ newborns. Numbers of apoptotic cells in *smFoxm1*$^{-/-}$, *Foxm1*$^{fl/fl}$ and *smMHC-Cre-GFP*$^{tg/-}$ lungs were counted in ten random 100x microscope fields. Mean ± S.D. was

determined using three different lungs in each group. A statistically significant p value < 0.05 is shown with asterisk.

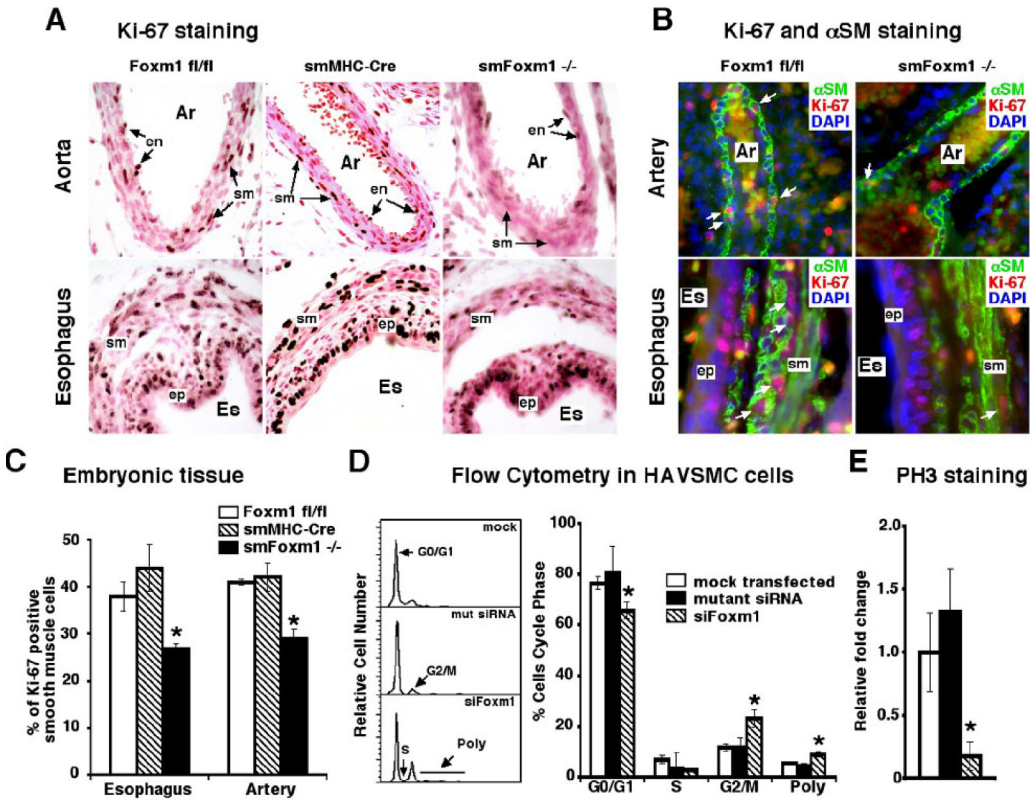

Figure 6. Diminished cellular proliferation in *smFoxm1*$^{-/-}$ smooth muscle cells

A-B, smFoxm1$^{-/-}$ embryos displayed diminished proliferation in smooth muscle cells. Paraffin sections from *smFoxm1*$^{-/-}$, *Foxm1*$^{fl/fl}$ and *smMHC-Cre-GFP*$^{tg/-}$ E18.5 embryos were stained with Ki-67 antibody (dark brown nuclei) and counterstained with nuclear fast red (A). In co-localization experiments (B), paraffin sections were stained with Ki-67 antibodies (red fluorescence), α-SM actin antibodies (green fluorescence) and DAPI (blue fluorescence). Erythrocytes displayed yellow autofluorescence. Diminished Ki-67 staining was selectively observed in smooth muscle cells (sm, shown with arrows) of *smFoxm1*$^{-/-}$ arteries (Ar) and esophagi (Es). Cellular proliferation was similar in endothelial (en) and epithelial cells (ep) of *smFoxm1*$^{-/-}$ and control *Foxm1*$^{fl/fl}$ embryos. Magnification is x400. *C, smFoxm1*$^{-/-}$ embryos exhibited a decreased number of Ki-67-positive smooth muscle cells. Percentages of Ki-67-stained smooth muscle nuclei were counted in ten random 400x microscope fields from *smFoxm1*$^{-/-}$, *Foxm1*$^{fl/fl}$ and *smMHCCre-GFP*$^{tg/-}$ E18.5 embryos. Mean ± S.D. was determined using three different embryos in each group. A statistically significant p value < 0.05 is shown with asterisk. *D*, Flow cytometry analysis of Foxm1-depleted HAVSMC cells shows decreased G0/G1 phase and accumulation of G2/M (4N) and polyploid cells (poly). HAVSMC cells were transfected with either siFoxm1 or mutant siRNA (siFoxm1) for 72 hours and then stained with propidium iodide and subjected to flow cytometry analysis. Graphically shown is the statistically significant change in the percentage of cells accumulating in G0/G1 and G2/M (4N) compared to mock-transfected cells. Means ± S.D. are calculated from triplicate plates. *E*, Foxm1 depletion diminishes the total number of HAVSMC cells undergoing mitosis. siRNA-transfected HAVSMC cells were immunostained with PH3 antibodies to visualize cells undergoing mitosis. Mock-transfected or mutant siRNA transfected HAVSMC cells were used as controls. Numbers of PH3-positive cells are presented as means ± S.D. from ten random x400 fields. Three cell cultures were used for each transfection.

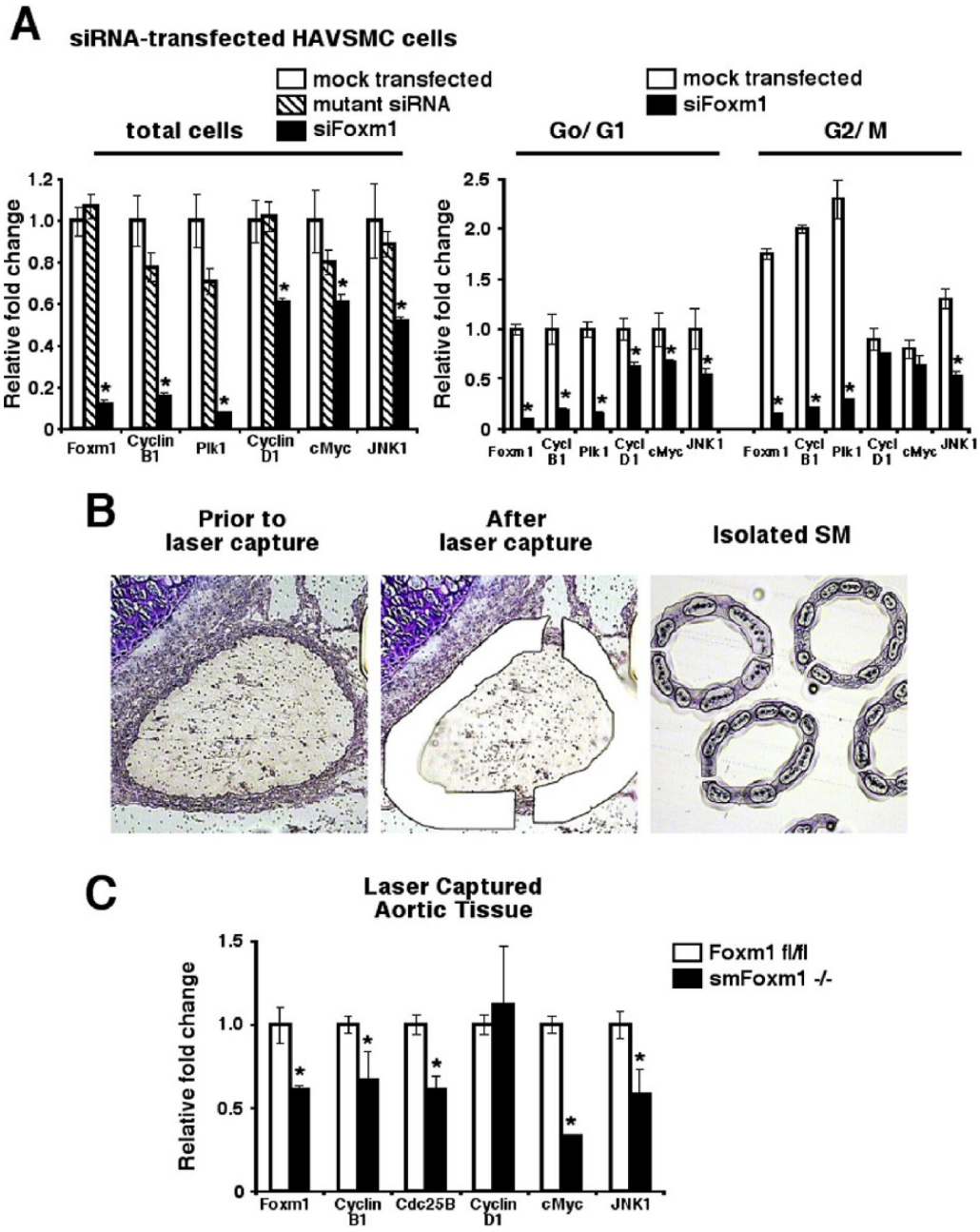

Figure 7. Foxm1-deficient smooth muscle cells displayed reduced expression of cyclin B1, c-Myc, JNK1 and Cdc25B phosphatase

A, siRNA transfection in HAVSMC cells shows decreased expression of cell cycle regulatory genes. HAVSMC cells were mock-transfected (control), transfected with siFoxm1 (siFoxm1) or transfected with mutant siRNA for 72 hours and then used for preparation of total RNA (left panel). In separate experiments, cells in G0/ G1 and G2/ M phases were isolated using flow cytometry and then used to prepare RNA (right panel). qRT-PCR shows decreased mRNAs of Foxm1, cyclins B1 and D1, Plk1, c-Myc and JNK1 kinase in siFoxm1 transfected cells. Each individual sample was normalized to its corresponding β-actin level. *B*, Images of frozen sections show isolation of aortic tissues of E16.5 embryos by a laser capture microdissection. *C*, Aortic tissues from *smFoxm1*$^{-/-}$ and control *Foxm1*$^{fl/fl}$ embryos were used for preparation of total RNA. qRT-PCR analysis was performed with primers specific to Foxm1, cyclins B1

and D1, c-Myc, JNK1 and Cdc25B phosphatase. Each individual sample was normalized to its corresponding β-actin level. Values are means ± S.D. A statistically significant p value < 0.05 is shown with asterisk.

Table 1

TaqMan gene expression assays (Applied Biosystems) were used for qRT-PCR analysis.

Mouse *TaqMan* gene expression assays	**Catalog Number**
Mouse Foxm1	Mm00514924_m1
Mouse Cyclin B1	Mm00838401_g1
Mouse Cdc25B	Mm00499136_m1
Mouse Cyclin D1	Mm00432359_m1
Mouse c-Myc	Mm00487804_m1
Mouse JNK1	Mm00489514_m1
Mouse Beta-Actin	Mm00607939_s1
Human Foxm1	Hs00153543_m1
Human Cyclin B1	Hs00259126_m1
Human Plk1	Hs00153444_m1
Human Cyclin D1	Hs00277039_m1
Human c-Myc	Hs00153408_m1
Human JNK1	Hs00177083_m1
Human Beta-Actin	Hs99999903_m1

Table 2

Breeding data for *smFoxm1*$^{-/-}$ mice

Developmental period	Total number of mice	Expected % of *smFoxm1*$^{-/-}$ mice	Experimental % (number) of alive *smFoxm1*$^{-/-}$ mice	% mortality in *smFoxm1*$^{-/-}$ mice
E15.5 –E16.5	36	50%	47% (17) (all alive)	0%
E17.5 – E18.5	75	50%	53% (40) (all alive)	0%
Postnatal day 1	98	50%	6% alive (6) 47% dead (46)	87%

Breeding data from smMHC-Cre GFP$^{tg/-}$ Foxm1$^{fl/fl}$ × Foxm1$^{fl/fl}$ mouse crosses are shown as a frequency of occurrence of smMHC-Cre GFP$^{tg/-}$ Foxm1$^{fl/fl}$ mice (*smFoxm1*$^{-/-}$).

Table 3

Functional Classification of up and down regulated genes

Term	Count	%	*P*-Value
Down-regulated genes			
GO:0007067~mitosis	38	22.22%	1.54E-37
GO:0000278~mitotic cell cycle	42	24.56%	2.12E-37
GO:0000087~M phase of mitotic cell cycle	38	22.22%	2.17E-37
GO:0022403~cell cycle phase	42	24.56%	2.33E-35
GO:0000279~M phase	39	22.81%	5.08E-35
GO:0007049~cell cycle	54	31.58%	1.67E-31
GO:0022402~cell cycle process	50	29.24%	7.05E-31
GO:0051301~cell division	33	19.30%	3.29E-29
GO:0000074~regulation of progression through cell cycle	26	15.20%	2.14E-12
GO:0051726~regulation of cell cycle	26	15.20%	2.42E-12
GO:0007017~microtubule-based process	15	8.77%	5.65E-09
Up-regulated genes			
GO:0048523~negative regulation of cellular process	10	19.61%	0.00174902
GO:0048519~negative regulation of biological process	10	19.61%	0.002343679
GO:0043066~negative regulation of apoptosis	5	9.80%	0.002670858
GO:0043069~negative regulation of programmed cell death	5	9.80%	0.002798642
GO:0032502~developmental process	16	31.37%	0.010578321
GO:0042981~regulation of apoptosis	6	11.76%	0.011146801
GO:0048468~cell development	9	17.65%	0.011636545
GO:0043067~regulation of programmed cell death	6	11.76%	0.011655337
GO:0006796~phosphate metabolic process	8	15.69%	0.014311992
GO:0008219~cell death	7	13.73%	0.017712167

Differentially expressed genes in siFoxm1-transfected HAVSMC cells were functionally classified according to Gene Ontology (GO). Gene Ontology analysis was performed using David (database for annotation, visualization, and integrated discovery).

Table 4

Gene expression profile of HAVSMC cells treated with Foxm1 specific siRNA

Gene Name	Genbank Number	siFoxm1 / control
Transcription factors and Cell cycle regulators		
forkhead box M1 (FoxM1)	NM_021953	0.10
centromere protein A	NM_001809	0.13
cyclin B1	N90191	0.14
protein regulator of cytokinesis 1	NM_003981	0.17
cyclin-dependent kinase inhibitor 3 (CDK2-associated dual specificity phosphatase)	AF213040	0.17
polo-like kinase 4 (Plk4)	AL043646	0.24
S-phase kinase-associated protein 2 (p45 or Skp2)	BG105365	0.25
CDC20 cell division cycle 20	NM_001255	0.27
cyclin A2	NM_001237	0.28
G-2 and S-phase expressed 1	NM_016426	0.28
cyclin E2	NM_004702	0.29
cell division cycle 2 (cdc2 or cdk1)	D88357	0.29
centromere protein F	NM_005196	0.30
aurora kinase B	AB011446	0.31
baculoviral IAP repeat-containing 5 (survivin)	BQ021146	0.31
polo-like kinase 1 (Plk1)	NM_005030	0.42
c-Jun N-terminal kinase (JNK1)	AB005663	0.45
c-Myc transcription factor	AY294976	0.50
Receptors, Structural and Intracellular signaling proteins		
CD36 antigen (collagen type I receptor, thrombospondin receptor)	W95035	0.20
retinoic acid receptor, alpha	AJ417079	0.20
calmodulin 1 (phosphorylase kinase, delta)	AI653730	0.29
interferon (alpha, beta and omega) receptor 1	AA811138	0.33
calcium/calmodulin-dependent protein kinase IV	*AL529104*	*5.3*
low density lipoprotein receptor-related protein 11	*AK021807*	*3.71*
Extracellular cell signaling and Secreted proteins		
a disintegrin and metalloproteinase domain 10	AU135154	0.33
placental growth factor	*BC001422*	*2.70*

HAVSMC cells were transfected with Foxm1-specific siRNA (siFoxm1) and then harvested at 72 hr after transfection. Total RNA was prepared from either siFoxm1 transfected or mock-transfected cells (3 cell cultures were used for each group) and then used for Affimetrix microarray. Values represent a fold change in RNA expression of siRNA-transfected cells compared to mock-transfected cells. Genes in normal type exhibited diminished expression in Foxm1-deficient cells, and genes in *italic type* displayed increased expression in Foxm1-deficient cells.